JOURNAL OF MATERIALS SCIENCE 37 (2002) 2413–2419

Preparation of SiC-based cellular substrate by pressure-pulsed chemical vapor infiltration into honeycomb-shaped paper preforms

Y. OHZAWA, K. NAKANE, V. GUPTA, T. NAKAJIMA
Department of Applied Chemistry, Aichi Institute of Technology, Yachigusa 1247, Yakusa-cho Toyota 470-0392, Japan
E-mail: ohzawa@ac.aitech.ac.jp

Using a pressure-pulsed chemical vapor infiltration technique, SiC was infiltrated from a $SiCl_4$ (4%)–CH_4 (4%)–H_2 gas phase into carbonized paper preforms at 1100°C. SiC-based cellular substrates with cell wall thicknesses of 25, 50 and 100 μm were obtained by using honeycomb-shaped paper preforms as the templates. The reduction of both wall thickness t and cell pitch d of SiC-based honeycomb substrate successfully led to an increase in geometric surface area per unit volume S, keeping pressure drop ΔP at constant, besides; ΔP decreased without lowering S by the reduction of t and the increase in d. The pressure drop in the prepared honeycomb substrates depended on $S^2\alpha^{-3}$ value, where α was open frontal area fraction. The compressive strength of the honeycomb substrates with t of 25 μm was about 7 MPa. The strength increased in proportion with $1-\alpha$, which corresponded to the volume fraction of the cell wall in the honeycomb substrate.

1. Introduction

Lightweight cellular ceramic substrates, so-called ceramic honeycomb substrates, are popular worldwide as the catalyst supports in, for example, automotive exhaust gas converters. In the honeycomb substrate design, reductions in the wall thickness increase the geometric surface area and decrease the heat capacity and pressure drop, leading to improved catalytic performance [1]. However, it is difficult to lower the thickness below 70–100 μm in the conventional ceramic substrate manufacturing processes, which involves extrusion of a slurry of the raw materials and sintering.

Recently, converting biological structures into synthetic materials has been of particular interest [2]. Sieber *et al.* reported a novel process for preparing cellular ceramics, which consisted of impregnation of low viscosity preceramic polymer suspensions into corrugated cardboard template preforms, and subsequent conversion to ceramic composites by pyrolysis [3]. This process offers another possibility for near net-shape manufacturing of lightweight ceramic honeycomb substrates.

In the last decade, the chemical vapor infiltration (CVI) technique has been developed for matrix filling of fiber preforms to produce fiber-reinforced ceramics [4, 5]. Amongst the CVI processes, three main methods have been developed; isothermal and isobaric CVI (ICVI) [6, 7], forced-flow CVI (FCVI) [8, 9] and pressure-pulsed CVI (PCVI). The PCVI method consists of repetition of the following steps of evacuation of the reaction vessel; instantaneous introduction of the source gas; and holding to allow deposition [10–13]. This process characteristically yields near net-shape products in relatively short operation times. Using the PCVI technique, it is expected that lightweight cellular ceramic substrates can be obtained by infiltrating a thin-walled corrugated paper preform. The matrix filling initiates from the half-thickness of the porous preform, then, propagates to the surface under suitable conditions [14, 15]. This indicates that the PCVI process is preferred for obtaining dense thin-wall structures, as the ceramic matrix can be deposited into the pores of the paper preforms before films are formed on the external surface of the preforms, stopping further densification.

As mentioned above, wall thickness reduction is effective in improving gas-permeability, however it may result in a decrease in mechanical strength. It is important to evaluate quantitatively the relationship between structural parameters and the properties of the catalyst support. In this study, novel SiC-based cellular substrates were synthesized by PCVI using carbonized papers as template preforms, and their properties as catalyst supports were investigated.

2. Experimental procedure

Board-shaped and honeycomb-shaped papers (Fig. 1) were used as the porous preforms. Board-shaped carbon preforms were prepared as follows. Three sorts of commercial paper having the different thicknesses were put between carbon plates, carbonized at 1000°C in Ar for 4 h, and cut to 10×15 mm^2. Honeycomb-shaped preforms were prepared as follows. Each paper

TABLE I Specific properties of preforms after carbonization

	Board-shaped preform		Honeycomb-shaped preform		
Type	Volume fraction of fiber	Porosity	Wall thickness, t (μm)	Cell pitch, d (mm)	Dimension (mm)
A	0.18	0.82	90–110	1.3	12 $\phi \times$ 30 long
B	0.15	0.85	45–55	1.2	10 $\phi \times$ 30 long
C-1	0.30	0.70	20–35	1.1	12 $\phi \times$ 30 long
C-2	0.30	0.70	20–35	1.5	13 $\phi \times$ 30 long

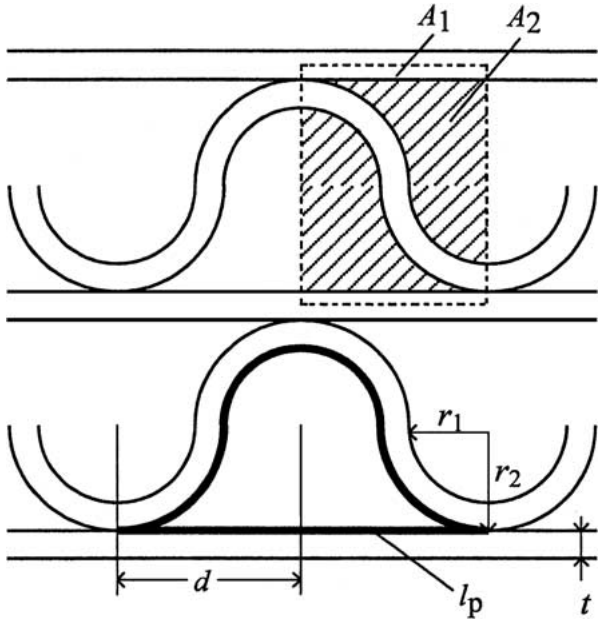

Figure 1 Schematic diagram of the cross-section of the honeycomb-shaped preform: d, cell pitch; t, wall thickness; lp, circumference of pore; A1, cross-section of unit cell; A2, cross-section of pore in unit cell.

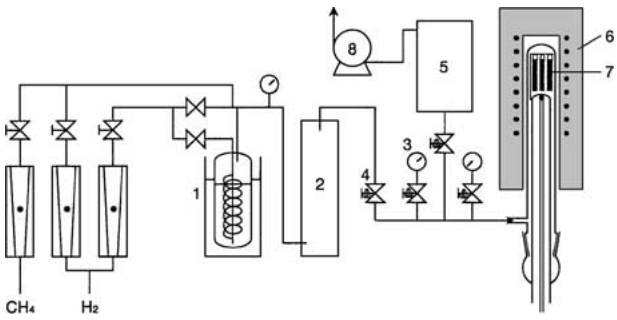

Figure 2 Apparatus for pressure pulsed chemical vapor infiltration of SiC: 1, $SiCl_4$ saturator; 2, reservoir; 3, pressure gauge; 4, electromagnetic valve; 5, vacuum tank; 6, furnace; 7, performs; 8, vacuum pump.

mentioned above was corrugated and rolled up using polyvinyl alcohol as the binder, carbonized under the same conditions as the board-shaped preforms, and cut to be 30 mm long. Fig. 1 shows a schematic diagram of the cross-section of the honeycomb-shaped preform and defines the structural parameters. Table I shows the initial porosity data of the board-shaped preforms, and the structural parameters of the honeycomb-shaped preforms.

The apparatus for PCVI of SiC is shown in Fig. 2. The source gas mixture of $SiCl_4$ (4%)–CH_4 (4%)–H_2 was allowed to flow into a reservoir. It was instantaneously introduced (within 0.1 s) into the reaction vessel up to a pressure of 0.1 MPa, and the pressure was held for 0.4 s to allow matrix deposition. Then, the gas was evacuated to below 0.7 kPa within 1.5 s. This cycle is one pulse, and it was repeated the desired number of times. The CVI temperature was kept at 1100°C.

The filling ratio was defined as the fraction of infiltrated SiC matrix (V_{sic}) per initial pore volume in the preform (V_{pore}), where V_{sic} and V_{pore} were estimated from the weight increase and the bulk density of the preform, respectively. Residual porosity (ε) of the sample was calculated from the following equation;

$$\varepsilon = \varepsilon_0[1 - (V_{sic}/V_{pore})] \quad (1)$$

where ε_0 is initial porosity of preform. In the calculation, the densities of the SiC deposits and preform carbon were assumed to be 3.1 and 1.8 g cm^{-3}, respectively.

Pressure drop was determined by measuring the air pressure for various air flow rates through a columnar sample in an axial direction at room temperature. Compressive strength along the axis was measured at room temperature using a Marusho 9004 mechanical testing machine. JSM-820 and JED-2000 (JEOL) microscopes were used for the scanning electron microscopy (SEM) and the electron probe microanalysis (EPMA), respectively.

3. Results and discussion

3.1. PCVI of SiC into board-shaped porous preforms

Using the board-shaped carbonized paper preforms with thicknesses of 100 μm (A-type), 50 μm (B-type) and 25 μm (C-type), SiC matrix infiltration was examined. The crystalline phase of the deposited matrix was identified as β-SiC from X-ray diffraction. Fig. 3 shows the SEM images of the ruptured cross-section of each preform after SiC infiltration. From Fig. 3a, c and e, it can be observed that SiC films with thicknesses of 0.5–1 μm are deposited around the carbonized fibers in the early stages of PCVI. Dense filling by the SiC matrix is achieved after 30000 pulses for A-type and B-type prefoms and 20000 pulses for the C-type preform, as shown in Fig. 3b, d and f, respectively. In Fig. 3f films have formed on the external surfaces of the preform. This prevents the penetration of the source gases into the preform, and stops further densification.

Fig. 4 shows the change in SiC filling ratio of the board-shaped preforms with number of pulses. For A-type and B-type preforms, the filling ratio increase up to 30000 pulses, after which it saturates at about 80%. Saturation of the filling ratio results from film

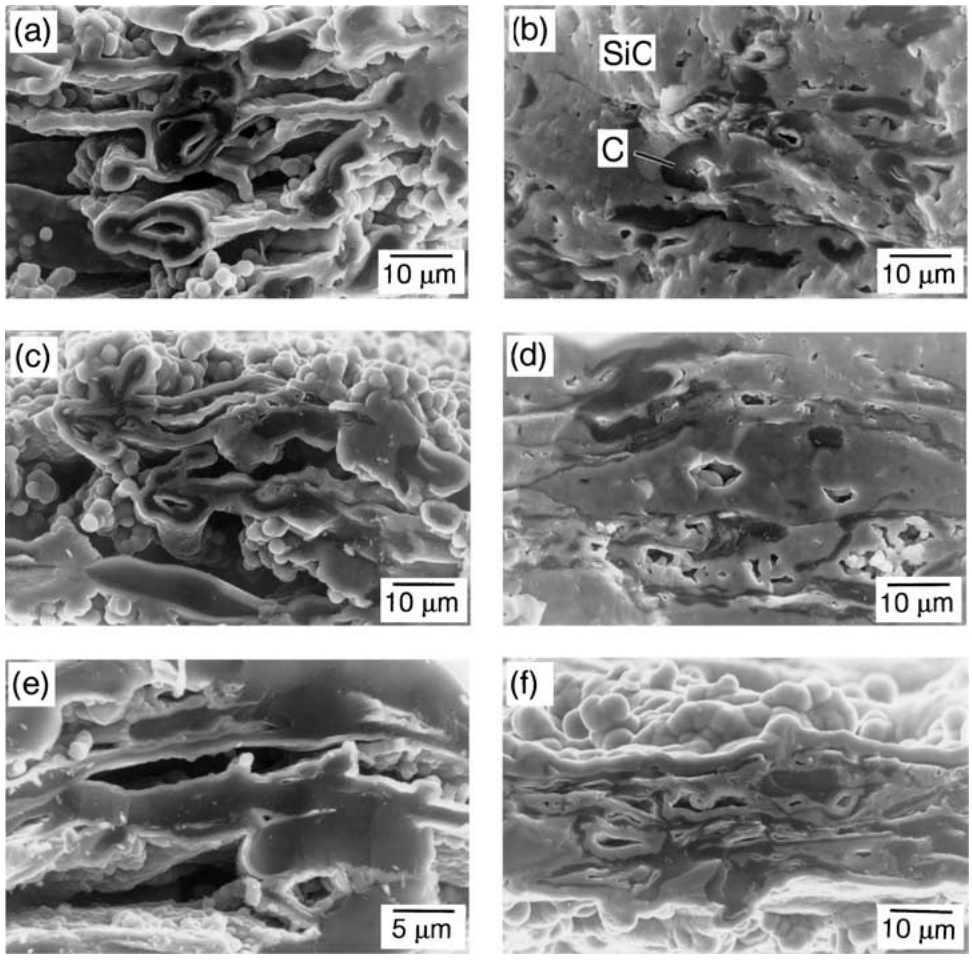

Figure 3 SEM images of ruptured cross-section of each preform after SiC infiltration; (a) and (b) A-type, (c) and (d) B-type, (e) and (f) C-type. Number of pulses; (a) and (c) 10000, (b) and (d) 30000, (e) 5000 (f) 20000.

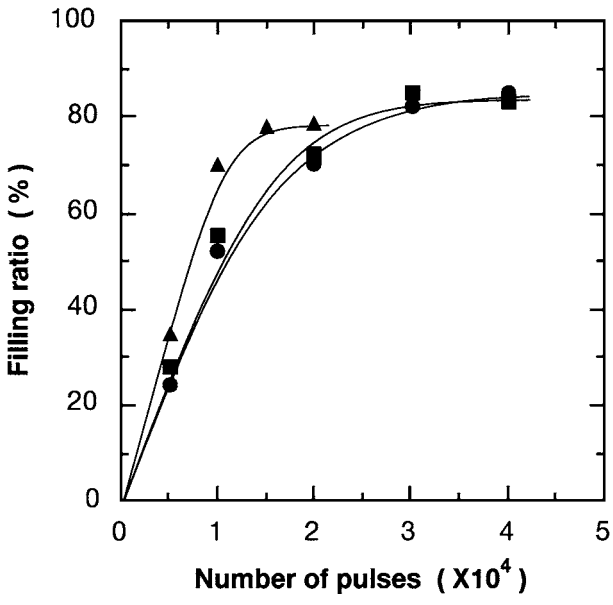

Figure 4 Change of SiC filling ratio of the board-shaped paper preforms with number of pulses; (■) A-type, (●) B-type, (▲) C-type.

formation on the external surfaces of the porous preforms. The saturation values of the filling ratio for the preforms are similar, however, C-type preform requires less pulses to reach this value because of the fiber volume fraction of this preform. As the area of fiber surface on which SiC film can be deposited increases with fiber volume fraction, a higher rate infiltration is achieved for the preform having the larger fiber volume fraction, assuming that the growth rate of SiC is constant. Table II shows the volume fractions of carbonized fiber, SiC matrix and residual porosity within A-type, B-type and C-type preforms after 30000, 30000 and 15000 pulses of PCVI, respectively. Residual porosity is constant at about 15%.

TABLE II Volume fraction of carbonized fiber, SiC matrix and residual porosity in the samples obtaind from the board-shaped paper preforms

Type	Carbonized fiber	SiC matrix	Pore
A	0.18	0.67	0.15
B	0.15	0.70	0.15
C	0.30	0.54	0.16

Number of pulses: A, 30000; B, 30000; C, 15000.

3.2. PCVI of SiC into honeycomb-shaped preforms

Fig. 5 shows the change in the deposited SiC weight with number of pulses for A-type, B-type and C1-type preforms. The increases in weight reach plateaus above 30000 pulses for A-type and B-type preforms, and above 15000 pulses for the C1-type preform. Fig. 6 shows SEM images and Si electron probe microanalysis (EPMA) maps of polished cross-sections of

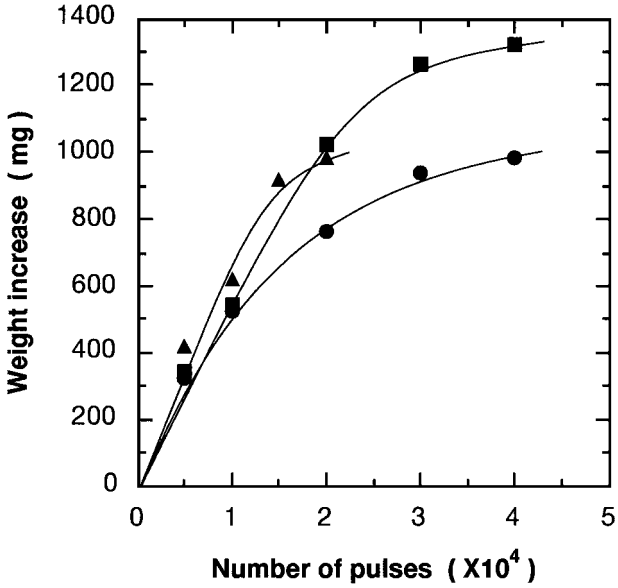

Figure 5 Change of SiC weight infiltrated into the honeycomb-shaped preforms with number of pulses; (■) A-type, (●) B-type, (▲) C1-type.

the honeycomb-shaped preforms after SiC infiltration. From low magnification images (a and b), it can be seen that the original shapes and sizes of the corrugated cell structures of the template preforms are retained after SiC infiltration. It appears that the cell walls adhere to each other in the both samples, and that the SiC has infiltrated uniformly.

3.3. Structural parameters and pressure drop in SiC-based honeycomb substrate

SiC-based honeycomb substrates were prepared by applying of 30000 pulses to A-type and B-type preforms, or 15000 pulses to C1 and C2-type preforms. Open frontal area fraction α and geometric surface area per unit volume S of the honeycomb substrates were obtained from the wall thickness t and the cell pitch d by using the following equations;

$$\alpha = \frac{A_1}{A_2} = \frac{d + (1 - \pi/2)t}{d + 2t} \tag{2}$$

and

$$S = \frac{l_p \cdot L}{A_1 \cdot L} = \frac{\pi + 2}{d + 2t}, \tag{3}$$

where A_1, A_2, l_p and L are cross-sectional area of the unit cell, cross-sectional area of a pore in the unit cell, circumference of a pore and length of honeycomb substrate, respectively. Table III shows the structural parameters of SiC-based honeycomb substrates along with the pressure drop (ΔP) data measured at a linear velocity of 5 ms^{-1} for a 30 mm long sample. Although ΔP values of A-type, B-type and C1-type substrates are similar, S is in the order C1-type > B-type > A-type substrate. Although S for the C2-type substrate

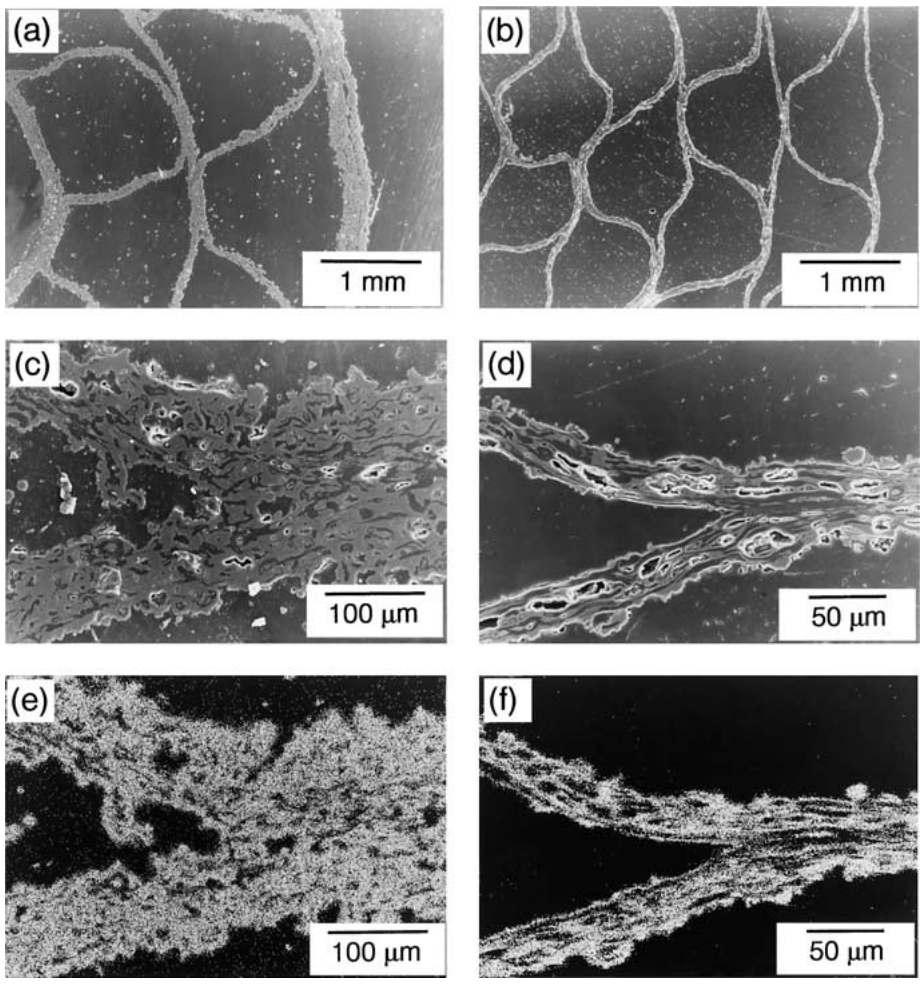

Figure 6 SEM images and EPMA Si maps of polished cross-sections of SiC honeycomb substrates: (a), (c) and (e) A-type preform; (b), (d) and (f) C1-type preform. (e) and (f) show EPMA Si maps of (c) and (d), respectively. Number of pulses: (a), (c) and (e) 30000; (b), (d) and (f) 20000.

TABLE III Structural parameters and pressure drop data of SiC honeycomb substrates

Type	Cell pitch, d (mm)	Wall thickness, t (μm)	Open frontal area fraction, α	Geometric surface area, S (m^2m^{-3})	$S^2\alpha^{-3}$ (m^{-2})	Pressure drop, ΔP[a]
A	1.3	90–110	0.83	3400	2100	110–120
B	1.2	45–55	0.90	4000	2200	120–130
C-1	1.1	20–35	0.94	4500	2300	100–120
C-2	1.5	20–35	0.96	3300	1300	60–80

[a]Measured at a linear velocity of 5 ms^{-1} for a 30 mm long sample.

is close to that of the A-type substrate, ΔP is about 40% lower. To relate ΔP to the structural parameters, Hagen-Poiseuille and Fanning's equation can be applied, which describes ΔP in a straight pipe for viscous flow;

$$\Delta P = \frac{32\mu L\bar{u}}{D^2}, \tag{4}$$

where μ, $\bar{u}$ and D are viscosity of the fluid, average velocity in the pipe and diameter of the circular pipe, respectively. For the present honeycomb structure, expressing D in Equation 4 as a hydraulic diameter D_p of a pore surrounded by the cell wall, which is defined as four times the cross-sectional area of the pore divided by the circumference of the cross-section of the pore, then Equation 5 is obtained;

$$D_p = \frac{4A_2}{l_p} = \frac{4A_2/A_1}{l_p/A_1} = \frac{4\alpha}{S}. \tag{5}$$

Next, applying the measurable velocity u_s in front of the honeycomb substrate instead of $\bar{u}$, Equation 6 is obtained;

$$\bar{u} = u_s/\alpha. \tag{6}$$

Combining Equations 4–6, the following relationship is derived;

$$\Delta P = \frac{2\mu u_s L S^2}{\alpha^3} \quad \text{or} \quad \Delta P\alpha\frac{S^2}{\alpha^3}. \tag{7}$$

Equation 7 indicates that ΔP is proportional to S^2/α^3 when u_s and L are constant. A-type, B-type and C1-type substrates have close S^2/α^3 values, so ΔP values are similar as shown in Table III. On the other hand, the decrease in S^2/α^3 value for C2-type substrate corresponds with a decreased ΔP.

ΔP can be related to cell pitch d and wall thickness t by substituting Equations 2 and 3 in Equation 7 to give:

$$\Delta P = \frac{2(\pi+2)^2\mu u_s L(d+2t)}{\{d+(1-\pi/2)t\}^3}. \tag{8}$$

Fig. 7 shows S and ΔP calculated from the several t and d values for the honeycomb substrate. The calculated ΔP of each substrate is close to the measured value shown in Table III. It is found that the reduction of both wall thickness t and cell pitch d leads to an increase in geometric area S, whilst keeping ΔP at constant. Alternatively, ΔP can be decreased without lowering S by a reduction in t and an increase in d.

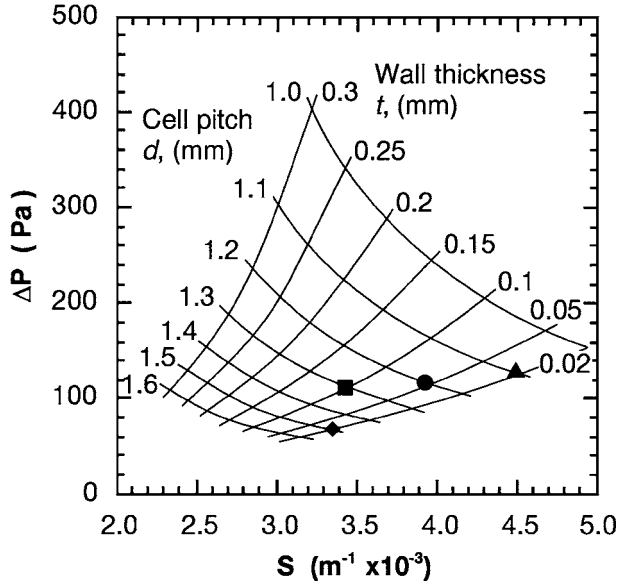

Figure 7 Pressure drop (ΔP) and geometric surface area per unit volume (S) calculated from wall thickness (t) and cell pitch (d) for the honeycomb substrate: sample length, 30 mm; linear velocity of air, 5 m s^{-1}. Preform; (■) A-type, (●) B-type, (▲) C1-type, (♦) C2-type.

3.4. Mechanical strength of SiC-based honeycomb substrate

Fig. 8 shows the change in compressive strength for A-type and C1-type preforms as a function of number of pulses. There is an increase in the strength with number of pulses until 30000 pulses for A-type and 15000 pulses for C1-type preforms. At these pulse numbers,

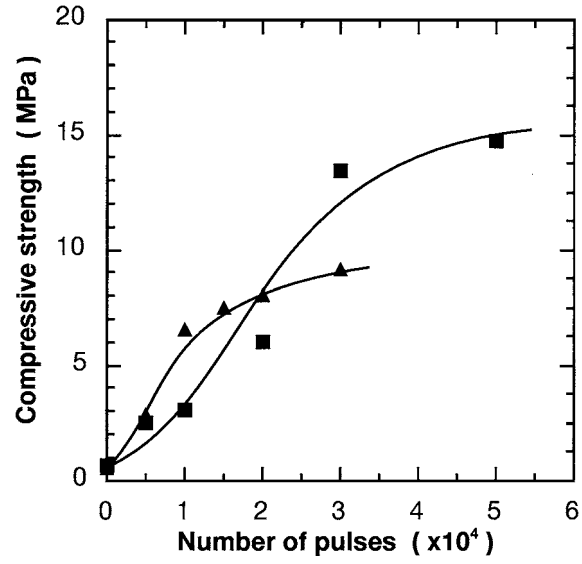

Figure 8 Change of compressive strength with number of pulses for (■) A-type and (▲) C1-type honeycomb-shaped preform.

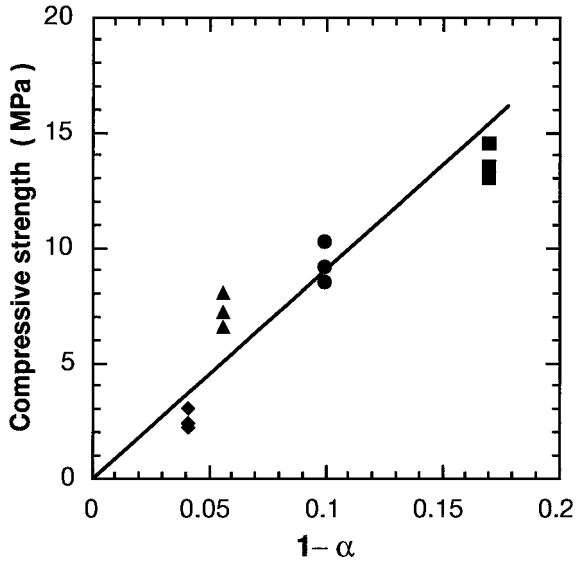

Figure 9 Relationship between the compressive strength and cross-sectional area fraction of cell wall in the honeycomb substrate ($1-\alpha$). Preform: (■) A-type, (●) B-type, (▲) C1-type, (♦) C2-type; number of pulses: (■) and (●) 30000, (▲) and (♦) 15000.

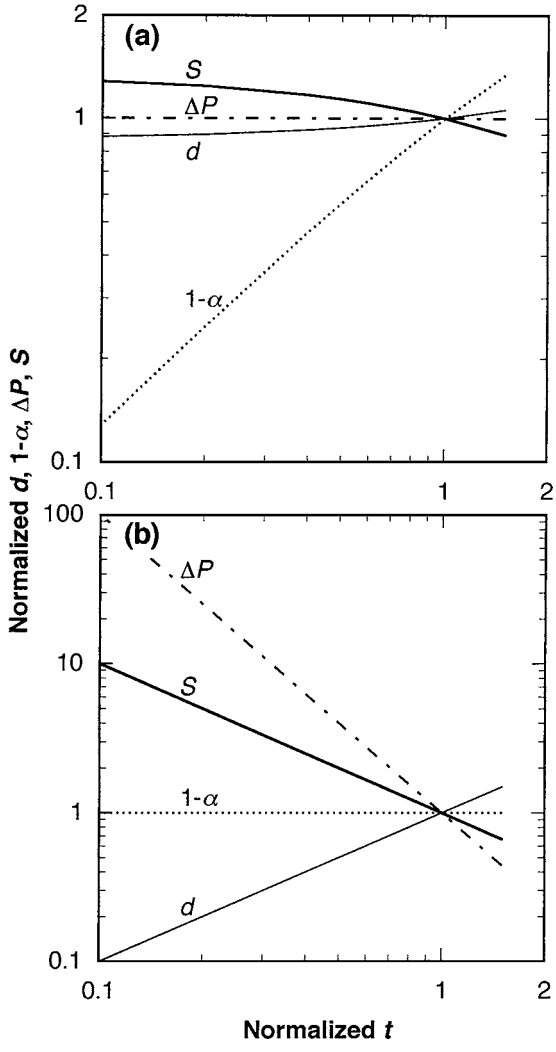

Figure 10 Cell pitch (d), cross-sectional area fraction of cell wall ($1-\alpha$), pressure drop (ΔP) and geometric surface area per unit volume (S) normalized with respect to the A-type sample as a function of wall thickness (t). Data plotted in (a) and (b) were calculated under constant ΔP and $1-\alpha$ conditions, respectively.

the SiC filling ratio saturates as shown in Fig. 4. This suggests that the strength is effectively increased by the densification of the cell wall rather than the formation of films on external surfaces. The strength of the A-type sample after saturation of the filling ratio is higher than that of the C1-type sample, commensurate with the difference in the volume fractions of cell walls in the honeycomb substrates. Fig. 9 shows the relationship between the compressive strength and the fraction of the cross-sectional area of the wall ($1-\alpha$), which corresponds to the volume fraction of the wall in the honeycomb structure. It is found that the strength increases linearly with $1-\alpha$ under the present conditions.

Using Equations 2, 3 and 8, $1-\alpha$ can be calculated from the wall thickness t and the cell pitch d along with the pressure drop ΔP and the geometric surface area S. Fig. 10 shows the calculated values of $1-\alpha$, ΔP and S as a function of d, where each value is normalized with respect to the values for the A-type substrate. From Fig. 10a, it is found that reducing the wall thickness t leads to an increase in S keeping ΔP constant. However, $1-\alpha$ decreases with t, which results in a decrease in strength. For the C1-type honeycomb substrate (normalized t of 0.25), the compressive strength is about 7 MPa. This value is somewhat lower than the reported value of 10 MPa for cordierite ceramic honeycomb substrates with a wall thickness of 150 μm in practical use [16]. It seems that further reduction of the wall thickness is undesirable with respect to the mechanical strength. On the other hand, to keep $1-\alpha$ constant (Fig. 10b), it is necessary to reduce the cell pitch d and t together. This produces a considerable increase in S, but, ΔP increases significantly.

4. Conclusions

Thin walled cellular ceramic substrates was prepared using PCVI of SiC from a $SiCl_4$ (4%)–CH_4 (4%)–H_2 gas phase into carbonized paper preform templates at 1100°C. Board-shaped and honeycomb-shaped template preforms were prepared from three sorts of papers having different thicknesses. The following conclusions were drawn from the present study.

1. SiC densely infiltrated the pores within the board-shaped preforms. Residual porosity decreased from 70–85% to 15% independent of the paper source.
2. SiC-based cellular substrates with the cell wall thicknesses of 25, 50 and 100 μm were obtained from the honeycomb-shaped preforms. The cell structures of the template preforms were retained in their original shape and size after SiC infiltration.
3. The reduction of both wall thickness t and cell pitch d of SiC-based honeycomb substrates led to an increase in the geometric surface area per unit volume S, whilst the pressure drop ΔP was constant, ΔP could be decreased without lowering S by reducing t and increasing d.
4. The pressure drop in the present honeycomb substrates appeared to follow the relationship derived from Hagen-Poiseuille and Fanning's equation, i.e., it depended on $S^2\alpha^{-3}$, where S and open frontal area fraction α were given as a function of t and d.

5. For the honeycomb substrate with t of 25 μm and d of 1.1 mm, the compressive strength was about 7 MPa. The strength increased linearly with $1-\alpha$, in accordance with increases in the volume fraction of the cell wall in the honeycomb substrate.

References

1. K. UMEHARA, T. YAMADA, T. HIJIKATA, Y. ICHIKAWA and F. KATSUBE, *SAE Paper* 971029 (1997) 115.
2. P. GALVERT, *Mater. Res. Soc. Bull.* **17** (1992) 36.
3. H. SIEBER, A. KAINDL, D. SCHWARZE, J. P. WERNER and P. GREIL, *CFI/Ber. DKG* **77** (2000) 21.
4. F. CHERISTIN, R. NASLAIN and C. BERNARD, in Proceedings of the 5th International Conference on CVD, edited by T. O. Sedgwick and H. Lyoltin (Electrochemical Society, New Jersey, 1979) p. 499.
5. I. GOLECKI, in Proceedings of the 13th International Conference on CVD, edited by T. M. Besmann, M. D. Allendorf, McD. Robinson and R. K. Ulrich (Electrochemical Society, New Jersey, 1996) p. 547.
6. R. NASLAIN, *J. Alloy Compd.* **188** (1992) 42.
7. O. P. S. DUGNE, A. GUETTE, R. NASLAIN, R. FOURMEAUX, Y. KHIN, J. SEVELY, J. P. ROCHER and J. COTTERET, *J. Mater. Sci.* **28** (1993) 3409.
8. T. M. BESMANN, R. A. LOWDEN, B. W. SHELDON and D. P. STINTON, in Proceedings of the 11th International Conference on CVD, edited by K. E. Spear and G. W. Cullen (Electrochemical Society, New Jersey, 1990) p. 482.
9. T. M. BESMANN, J. C. McLAUGHLIN and H. T. LIN, *J. Nucl. Mater.* **219** (1995) 31.
10. K. SUGIYAMA and T. NAKAMURA, *J. Mater. Sci. Lett.* **6** (1987) 331.
11. F. LANGLAIS, P. DUPEL and R. PAILLER, in Proceedings of the 13th International Conference on CVD, edited by T. M. Besmann, M. D. Allendorf, McD. Robinson and R. K. Ulrich (Electrochemical Society, New Jersey, 1996) p. 555.
12. H. J. JEONG, H. D. PARK, J. D. LEE and J. O. PARK, *Carbon* **34** (1996) 417.
13. Y. OHZAWA, M. TAKAHASHI and K. SUGIYAMA, *J. Mater. Sci.* **32** (1997) 4289.
14. K. SUGIYAMA and Y. OHZAWA, *ibid.* **24** (1989) 3756.
15. J. Y. OFORI and S. V. SOTIRCHOS, *J. Mater. Res.* **11** (1996) 2541.
16. J. KITAGAWA, *Industrial Mater.* **38** (1990) 49 (in Japanese).

Received 6 September 2001
and accepted 14 February 2002